MICROCOPY RESOLUTION TEST CHART

BUREAU OF STANDARDS-1963-A

④

AD-A193 749

OFFICE OF NAVAL RESEARCH

Contract N00014-83-K-0470-P00003

Task No. NR 359-718

TECHNICAL REPORT # 64

Electrolyte Effects on the Cyclic Voltammetry of TCNQ and TCNE

By

Stanley Pons, S. Khoo, J. Foley

University of Utah
Department of Chemistry
Salt Lake City, Utah 84112

DTIC
ELECTE
APR 1 3 1988
S   D
∞H

July 30, 1986

88   4   12   863

REPORT DOCUMENTATION PAGE		READ INSTRUCTIONS BEFORE COMPLETING FORM
1. REPORT NUMBER 64	2. GOVT ACCESSION NO.	3. RECIPIENT'S CATALOG NUMBER
4. TITLE (and Subtitle) Electrolyte Effects on the Cyclic Voltammetry of TCNQ and TCNE		5. TYPE OF REPORT & PERIOD COVERED Technical Report # 64
		6. PERFORMING ORG. REPORT NUMBER
7. AUTHOR(s) Stanley Pons, S. Khoo, J. Foley		8. CONTRACT OR GRANT NUMBER(s) N00014-83-K-0470-P0003
9. PERFORMING ORGANIZATION NAME AND ADDRESS University of Utah Department of Chemistry Salt Lake City, UT 84112		10. PROGRAM ELEMENT, PROJECT, TASK AREA & WORK UNIT NUMBERS Task No. NR 359-718
11. CONTROLLING OFFICE NAME AND ADDRESS Office of Naval Research Chemistry Program - Chemistry Code 472 Arlington, Virginia 22217		12. REPORT DATE July 30, 1986
		13. NUMBER OF PAGES
14. MONITORING AGENCY NAME & ADDRESS(if different from Controlling Office)		15. SECURITY CLASS. (of this report) Unclassified
		15a. DECLASSIFICATION/DOWNGRADING SCHEDULE

16. DISTRIBUTION STATEMENT (of this Report)

This document has been approved for public release and sale; its distribution unlimited.

17. DISTRIBUTION STATEMENT (of the abstract entered in Block 20, if different from Report)

18. SUPPLEMENTARY NOTES

19. KEY WORDS (Continue on reverse side if necessary and identify by block number)

TCNE, TCNQ, Cyclic Voltammetry

20. ABSTRACT (Continue on reverse side if necessary and identify by block number)

The electrochemistry of TCNQ and TCNE is discussed.

DD FORM 1473 JAN 73 1473   EDITION OF 1 NOV 65 IS OBSOLETE
S/N 0102-LF-014-6601

ELECTROLYTE EFFECTS ON THE
# CYCLIC VOLTAMMETRY OF
TCNQ AND TCNE

S.B. Khoo[*], John. K. Foley, and Stanley Pons[**]
Department of Chemistry
University of Utah
Salt Lake City, UT 84112

*Present address: Department of Chemistry
National University of Singapore
Kent Ridge
Singapore 0511

** To whom correspondence should be addressed.

INTRODUCTION

In aprotic solvents the electrochemical reduction of tetracyanoquinodimethane (TCNQ) and tetracyanoethylene (TCNE) takes place in two distinct one-electron steps;

$$R + e^- \rightleftarrows R^{\bar{}} \tag{1}$$

$$R^{\bar{}} + e^- \rightleftarrows R^{2-} \tag{2}$$
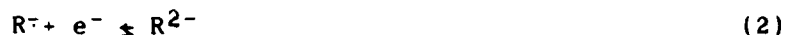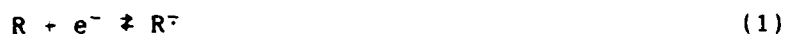
A radical anion is formed in the first step, and at much more negative potentials a further electron transfer takes place to form a dianion. The first reduction step of TCNE and both reduction steps of TCNQ are very fast [1-5]. The radical anions and dianions are stable in aprotic and oxygen-free solutions [1,6,7], except that the dianions and neutral molecules can reproportionate to form two radical anions.

$$R^{2-} + R \rightleftarrows 2R^{\bar{}} \tag{3}$$

In this note we report a study by cyclic voltammetry of the reductions of TCNQ and TCNE to their radical anions and dianions at platinum and glassy carbon electrodes in acetonitrile. We emphasize the effect of different supporting electrolyte cations on the voltammetry because (a) there exists the possibility of ion-pairing between the dianions and small cations [8-15], and (b) it appears that the rates of some electron transfer reactions depend on supporting electrolyte [6,10,16-26]. For example, at a platinum electrode in acetonitrile, the voltammetric wave at 100 mV s^{-1} for reduction of TCNE$^{\bar{}}$ to TCNE^{2-} is reversible with LiClO$_4$ as the supporting electrolyte [16,17], but quasireversible with tetra-n-butylammonium perchlorate (TBAP) [6] or tetra-n-butylammonium fluoroborate (TBAF) [16] as supporting electrolyte.

EXPERIMENTAL

Cells and instrumentation

A standard three-electrode cell was used. The reference electrode was a silver wire in contact with an acetonitrile solution of $AgNO_3$ (0.01 M) and 0.1 M of the same supporting electrolyte as in the cell. The secondary electrode material was platinum. Working electrodes were fabricated from platinum and carbon; the platinum electrode was a wire sealed into glass and the carbon electrode was a glassy carbon disc made by sealing a piece of glassy carbon rod (3 mm diameter, Tokai) into glass tubing with epoxy and polishing the end to a mirror finish with alumina on a polishing cloth. The areas of the two electrodes were found from current-time transients taken during the diffusion-controlled reduction of anthracene in acetonitrile. From the Cottrell equation, taking the diffusion coefficient of anthracene in acetonitrile to be 2.55×10^{-5} cm^2s^{-1} [27], the area of the platinum wire was found to be $0.227(\pm0.016)$ cm^2 and that of the glassy carbon disc was found to be $0.094(\pm0.005)$ cm^2.

The potential of the working electrode with respect to the reference electrode was controlled with a HiTek DT2101 potentiostat and a HiTek PPR1 waveform generator. Cyclic voltammograms were recorded on a Linseis LX1000 chart recorder. Positive feedback was used to reduce the iR drop between the tip of the Luggin capillary and the working electrode; in no experiment was the scan rate greater than 600 mV s^{-1}, and under these circumstances it was estimated that the iR loss was no more than the error in reading potentials from the recorded voltammograms (±5 mV).

Before each experiment the solution was deaerated by bubbling purified nitrogen through the cell. All experiments were carried out at room temperature, which was $23.0(\pm 0.5)^{O}C$. All potentials in this paper are given with respect to the Ag/Ag^{+} (0.01 M) reference electrode, unless otherwise stated.

Chemicals.

Reagent grade lithium and sodium perchlorates were recrystallized twice from triply distilled water. Tetra-n-butylammonium fluoroborate (TBAF) was prepared according to the method of Lund and Iverson [28] and recrystallized from methylene chloride and ice-cooled anhydrous ether and then from methylene chloride and distilled water. Tetraethylammonium perchlorate (TEAP) (Eastman, reagent grade) was recrystallized twice from triply distilled water. Reagent grade TCNE (Eastman) was recrystallized twice from chlorobenzene. Reagent grade TCNQ (Eastman) was recrystallized twice from acetonitrile [29]. The dried crystals of TCNE melted at $200-201^{O}C$ and those of TCNQ melted at $294-295^{O}C$, in agreement with literature values [4]. Acetonitrile (Caledon HPLC grade, water content nominally 0.005%) was dried over Woelm neutral alumina (Supergrade I) before use.

RESULTS

Reduction of TCNQ

Cyclic voltammograms were run for acetonitrile solutions of TCNQ (1 mM) at platinum and glassy carbon electrodes, using TBAP, TEAP, $NaClO_4$ and $LiClO_4$ as supporting electrolytes. The sweep rate, v, was varied between 25 mV s^{-1} and 500 mV s^{-1}. Figure 1 shows representative cyclic voltammograms run at the carbon electrode. The voltammograms run at platinum were similar. Peak potentials, E_{pc} and E_{pa}, and peak separations, ΔE_p, for the first and second reduction waves are given in Table 1.

At these sweep rates the first reduction wave of all seven systems showed simple reversible behavior according to the usual criteria: the cathodic and anodic peak potentials were independent of sweep rate and were separated by 60 to 70 mV, which is close to the theoretical value of 59 mV for a reversible one-electron reduction; the ratio of the anodic to cathodic peak currents, i_{pa}/i_{pc}, was close to 1.0 for all systems; the ratio $i_{pc}/v^{\frac{1}{2}}$ was approximately independent of sweep rate v. The cathodic and anodic peak potentials were independent of electrode material and electrolyte, and the half-wave potential, $E_{1/2}$, was about -0.11 V. From the Randles-Sevcik equation for a reversible process

$$i_{pc} = 2.69 \times 10^5 \; n^{3/2} \; A \; C_0 \; D_0^{1/2} \; v^{\frac{1}{2}} \tag{4}$$

the diffusion coefficient, D_0, of TCNQ was measured at $1.6(\pm0.2) \times 10^{-5}$ cm^2 s^{-1}. This value was independent of the supporting

electrolyte and agrees quite well with the value of 1.42×10^{-5} cm^2 s^{-1} measured by Sharp [6].

When considering the second reduction wave of TCNQ we assume that the homogeneous reproportionation reaction (3) can be ignored and that therefore the half-wave potentials measured from the second wave are those for the TCNQ$^-$/TCNQ^{2-} couple. This is rigorously true only if the diffusion coefficients of TCNQ, TCNQ$^-$, and TCNQ^{2-} are equal and if the second wave is reversible: under these circumstances reaction (3) has no effect on the current [30] but if the second electron transfer is slow then the effect of reaction (3) is to reduce the current [31]. For the systems discussed here, however, with slow sweep rates and well separated voltammetric waves, it is likely that at potentials in the second wave the amount of neutral TCNQ or TCNE close to the electrode has decreased to a very small value, in which case, irrespective of equality of diffusion coefficients or the rate of heterogeneous electron transfer, reaction (3) does not take place sufficiently close to the electrode to affect the current.

The second reduction wave also fulfilled the above criteria for reversibility. For example, the cathodic and anodic peak potentials were independent of sweep rate and electrode material and were 60 to 70 mV apart. From equation (4), ignoring reproportionation, the diffusion coefficient of TCNQ$^-$ was measured as $1.4(\pm0.2) \times 10^{-5}$ cm^2 s^{-1}, a value slightly lower than that of TCNQ.

An important difference between the first and second waves, however, was that the peak potentials of the second wave were dependent upon the supporting electrolyte. The half-wave potentials of the

second electron-transfer were -0.66 V with TBAF (0.1 M) and TEAP (0.1 M) as supporting electrolytes, -0.63 V with $NaClO_4$ (0.1 M), and -0.52 V with $LiClO_4$ (0.1 M). We attribute this to ion-pairing between the dianion formed in the second wave and alkali metal cations. Such an interaction would lower the free energy of the electron-transfer reaction by stabilizing the product of the reaction, and the reduction would take then place at less negative potentials. The positive shift in half-wave potential should increase with the strength of ion-pairing and with the concentration of ion-pairing cations [11-15]. Indeed TCNQ solutions with mixtures of TBAF and $MClO_4$ as electrolyte showed this behaviour; there were two reversible waves as before, and the more negative one shifted positive as the metal cation concentration was increased.

Reduction of TCNE

Cyclic voltammograms of 1.00 mM solutions of TCNE with TEAP, TBAF, $LiClO_4$, and $NaClO_4$ as supporting electrolytes were run at sweep rates ranging from 25 mV s^{-1} to 600 mV s^{-1} at the platinum and glassy carbon electrodes. Figure 2 shows representative cyclic voltammograms run at the carbon electrode. Peak potentials and peak separations for both reduction waves are given in Table 2. For all eight systems the first reduction wave showed reversible behavior and the half-wave potential was about -0.07 V. The diffusion coefficient of TCNE was calculated from equation (4) to be 1.9($\pm$0.2) x 10^{-5} cm^2 s^{-1}. This value, which was independent of electrolyte, agrees well with the literature value of 1.91 x 10^{-5} cm^2 s^{-1} [4].

From Figu : 2 and Table 2 it is apparent that, unlike the second reduction wa e of TCNQ, the second reduction wave of TCNE is not reversible for all supporting electrolytes and the peak potentials are not independent of electrode material. The four supporting electrolytes fall into two groups; $NaClO_4$ and $LiClO_4$ give nearly reversible behavior which is independent of the electrode material, while TBAF and TEAP give irreversible behavior and the irreversibility is greater at a platinum electrode than at a carbon electrode. In addition, the peak potentials become less negative as the radius of the cation of the supporting electrolyte decreases, indicating that contact ion-pairs are formed between $TCNE^{2-}$ and the electrolyte cation, just as for $TCNQ^{2-}$. (Once again we assume that the reproportionation reaction can be ignored, either because the diffusion coefficients of TCNE, $TCNE^{-}$, and $TCNE^{2-}$ are equal and the second wave is reversible, or because there is no neutral TCNE close to the electrode at potentials in the second wave and the only process taking place is reduction of $TCNE^{-}$ to $TCNE^{2-}$. The validity of this assumption was checked by interrupting the sweep for 60s at a potential between the two waves, and it was found that this did not affect the peak potentials of the second wave).

In the presence of $NaClO_4$ and $LiClO_4$ the peak potentials of the second reduction wave were independent of electrode material. The peak separations were not far from the 59 mV expected for a reversible one-electron process and not very dependent on sweep rate. At the platinum electrode i_{pa}/i_{pc} values for the second wave were close to 1.0 with $NaClO_4$ and $LiClO_4$ as electrolytes. At the carbon electrode

i_{pa}/i_{pc} was 1.0 when $NaClO_4$ was the electrolyte, but varied with sweep rate (from 1.29 at 50 mV s^{-1} to 1.52 at 300 mV s^{-1}) when $LiClO_4$ was the electrolyte. The ratio $i_{pc}/\nu^{\frac{1}{2}}$ was approximately constant at different sweep rates and 10-15% smaller than for the first wave.

In the presence of TBAF and TEAP the separation between the anodic and cathodic peaks of the second wave was much larger than 59 mV and increased with increasing sweep rate, indicative of an irreversible process. Furthermore, the electron transfer was more irreversible in the presence of TBAF than in the presence of TEAP and more irreversible at the platinum electrode than at the carbon electrode. The ratio $i_{pc}/\nu^{\frac{1}{2}}$ was roughly constant and again 10-15% lower than the value for the first wave. In the presence of TBAF and TEAP the electrode kinetics of the second wave are slow enough to allow the standard heterogeneous rate constant, k_s, to be determined for the reduction of $TCNE^-$ For the systems TBAF/C, TEAP/C, and TEA/Pt, k_s was calculated from the variation of peak separation, ΔE_p, with sweep rate, ν, using the method of Nicholson [32] for a quasi-reversible electron transfer reaction. The resulting k_s values are shown in Table 3. (These values did not vary significantly with sweep rate). The second wave of the TBAF/Pt system was assumed to be completely irreversible and the relationship between cathodic half-peak potential and sweep rate for an irreversible electron-transfer reaction (equation (5)) was used [33].

$$E_{p/2} = E° + (RT/\alpha nF) \{\ln(k_s/D_0^{\frac{1}{2}}) + \tfrac{1}{2}\ln(RT/\alpha nF) + 1.077 - \tfrac{1}{2}\ln \nu\} \qquad (5)$$

(The half-peak potential, $E_{p/2}$, was measured instead of E_p because the

wave was rather broad). $E_{p/2}$ was plotted against ln ν. The slope gave the cathodic charge-transfer coefficien $\cdot = 0.35$. The intercept gave $k_s = 7 \times 10^{-6}$ cm s^{-1}, assuming that E^o, the standard potential of the irreversible TCNE$^-$/TCNE^{2-} couple in TBAF/acetonitrile, was equal to the half-wave potential of the quasi-reversible couple in TEAP/acetonitrile, which was -1.05 V. (This assumes negligible ion-pairing between TEA$^+$ and TCNE^{2-}, which seems reasonable in view of the lack of ion-pairing between TEA$^+$ and TCNQ^{2-}).

Reduction of TCNE in the presence of mixed electrolytes gave more complicated behavior then did reduction of TCNQ (Figure 3). As can be seen from this figure, the reduction of TCNE was not affected by mixtures of different supporting electrolytes and different electrode materials; the criteria for electrochemical reversibility were still obeyed by the first wave. Reduction of TCNE$^-$ in mixed electrolytes, however, showed sharp symmetric waves at both electrodes suggestive of adsorption or phase deposition processes. For example, with 0.095 M TBAF and 0.005 M LiClO$_4$ at a platinum electrode, the reverse wave at -0.8 V appeared to be an adsorption peak. For 0.05 M TEAP and 0.05 M LiClO$_4$ at platinum, the reverse wave also appeared to be an adsorption peak, but was shifted positive to -0.2 V. In the case of 0.05 M TBAF and 0.05 M LiClO$_4$ at carbon, a prepeak was observed on the forward sweep and the reverse wave was again quite sharp. Such adsorption or deposition did not appear to occur in the reductions of TCNQ and TCNQ$^-$.

DISCUSSION

The half-wave potentials, taken to be the mean of the cathodic and anodic peak potentials, for the reductions of TCNQ and TCNE are summarized in Table 3. This Table also shows the standard heterogeneous rate constants for the reduction of $TCNQ^{-}$ and $TCNE^{-}$ at carbon and platinum, and the rate constants at platinum after a Frumkin correction [34] for the potential drop ϕ_2 between the outer Helmholz plane (OHP) and the solution. The charge density on the electrode, necessary to calculate ϕ_2, was found for $LiClO_4$ and $NaClO_4$ in acetonitrile at platinum by integrating capacitance-potential curves from reference [35] between the potential of zero charge (pzc) and the half-wave potential. (For platinum in acetonitrile the pzc is -0.42 V vs. $Ag/Ag^{+}(0.01$ M) [35] and at high concentrations (~ 0.1 M) the capacitance is constant at 3 μF cm^{-2} between the pzc and potentials used here). Frumkin corrections for the other electrolytes were assumed to be the same as for $LiClO_4$ and $NaClO_4$, though they may in fact be somewhat less.

Half-wave potentials

The half-wave potentials of the first reduction waves of both TCNQ and TCNE are independent of electrolyte, indicating that alkali metal cations do not form strong ion pairs with either $TCNQ^{-}$ or $TCNE^{-}$ in acetonitrile.

The half-wave potentials of the second waves show that both $TCNQ^{2-}$ and $TCNE^{2-}$ are stabilized by ion pairing with alkali metal cations; when the large organic cations of the supporting electrolyte are

replaced by Na^+ or Li^+ there is a positive shift in $E_{1/2}$ as $\Delta G°$ for reaction (2) becomes more negative. Both dianions are stabilized by Li^+ more than by Na^+; this indicates that contact ion-pairs rather than solvent-separated ion-pairs are formed. The shifts in $E_{1/2}$ due to ion pairing are larger for the $TCNE^-/TCNE^{2-}$ couple than for the $TCNQ^-/TCNQ^{2-}$ couple, as expected from the smaller size of $TCNE^{2-}$.

$E_{1/2}$ for reduction of TCNE is only slightly less negative than $E_{1/2}$ for reduction of TCNQ, in agreement with literature data [36] but, for a given electrolyte, $E_{1/2}$ for $TCNE^-$ reduction is considerably more negative than $E_{1/2}$ for $TCNQ^-$ reduction. Presumably repulsion between the two extra electrons is greater in $TCNE^{2-}$ than in the larger pi-system of $TCNQ^{2-}$.

Rate Constants

The first reduction steps were reversible in all electrolytes and at both electrode materials. The largest peak separation at 100 mV s^{-1} sweep rate was 72 mV, which means that k_s for the first electron transfer was greater than 3×10^{-2} cm s^{-1} in all cases. This is consistent with Sharp's data for platinum (k_s = 0.260 cm s^{-1} for TCNQ reduction and k_s = 0.159 cm s^{-1} for TCNE reduction [5]), but not with his data for carbon (k_s = 0.0035 cm s^{-1} for TCNQ reduction and k_s = 0.0021 cm s^{-1} for TCNE reduction [4]). The discrepancy might arise from the different types of carbon used; glassy carbon in this work and wax-impregnated graphite in reference [4].

The rate constants for $TCNQ^-$ reduction in the presence of TEAP and TBAP are faster than the corresponding rate constants for $TCNE^-$

reduction even after the differences in ϕ_2 potentials are taken into account. This might be due to a high inner reorganization energy for formation of $TCNE^{2-}$ if the dianion is not planar [6].

Increasing cation size decreases the standard rate constant for reduction of $TCNE^{-}$. This has also been observed for reductions in several other aprotic systems [10,19-26]. Several explanations for such behaviour are possible. One possibility is blockage of the electrode surface, for example by specific adsorption of tetraalkylammonium cations, or by strong adsorption of $TCNE^{-}$ or $TCNE^{2-}$ in the presence of TBAF and TEAP, or by deposition of tetraalkylammonium salts of $TCNE^{2-}$. This seems unlikely, however, because voltammograms of mixtures of TCNE and anthracene in the presence of TBAF show reversible reduction of anthracene at potentials more negative than the irreversible second wave of TCNE, and likewise voltammograms of mixtures of TCNE and TCNQ in the presence of TBAF showed reversible reduction of $TCNQ^{-}$ at potentials between the two waves of TCNE. Furthermore, with pure TEAP or TBAF as electrolytes no direct evidence for adsorption of the anion or dianion (such as prepeaks on the forward sweep, sharp peaks on the reverse sweep [37]) was observable (Figure 2).

It is probable, then, that the reduction processes observed here are all simple outer sphere electron transfers. Ion-pairing with the electrolyte cation might play a role in keeping the TCNE dianion planar, thereby reducing the reorganization energy for its formation, but it is difficult to envisage exactly how this could occur. It is more likely, as proposed for similar systems [10,19,23-25], that the

cation effect arises from a variation in the position of the outer Helmholz plane (OHP) with cation size, which can affect the rate of an outer sphere electron transfer reaction in a number of ways.

Effect of OHP Position

The outer Helmholz plane is the plane of closest approach of electrolyte ions to the electrode surface. According to the simple GCS model [34], there is a linear potential drop across the inner layer between the metal and OHP, if there is no specific adsorption, and a roughly exponential potential drop across the diffuse part of the double layer between the OHP and the bulk solution. At potentials well negative of the pzc nearly all of the ions at the OHP will be cations, and therefore the electrode-OHP distance will increase with size of the cation. It is usually assumed that electron transfer takes place with the reactant at the OHP. (The Frumkin correction depends upon this assumption).

Russel and Jaenicke [10,19] have attributed the effect of increasing cation size to decrease in electros·.cic interaction between the reacting species and its image charge in the electrode, which would increase the outer sphere reorganization energy for electron transfer. Others have suggested, however, that image forces are negligible because of screening by electrolyte between the reactant and electrode [38,39], and there is some experimental evidence for this [40,41].

Fawcett [23,25] and Corrigan and Evans [24], have pointed out that the reaction site need not be at the OHP, but might be anywhere in the inner layer or diffuse layer. Assuming the potential of the metal and

of the OHP to be fixed, at potentials negative of the pzc the potential ϕ_r at this reaction site must become more negative, and hence the rate of reduction lower, with increasing metal-OHP distance.

Another possibility is nonadiabaticity. Any electron transfer must become non-adiabatic when the electrode-reactant separation is large enough, and for non-adiabatic homogeneous electron transfers there is considerable evidence that the rate of electron transfer decreases exponentially with increasing separation of the reactants [42-44]. In fact it appears that most homogeneous electron transfer reactions between transition metal complexes are either marginally or completely nonadiabatic [42-44]. If this is also true for reactions at electrodes, as suggested by Hupp and Weaver [45-47], then approximately

$$k_s = k_{s0}\exp[-\gamma(r-r_0)] \qquad (6)$$

where r is the electrode-reactant separation. r_0 is the value of r at the plane of closest approach of the reactant, and k_{s0} is the value of k_s at this point. The coefficient γ has been estimated to lie in the range 1-2 A^{-1} [42-44].

Clearly if a nonadiabatic electron transfer takes place at the OHP the probability of electron transfer should decrease with increasing distance between the metal and the OHP. Differences in electron transfer rates between Cr(III) complexes have been explained in a similar manner by one complex being able to approach more closely than another to the electrode surface [47]. In practice, the reaction site (or range of sites) is expected to be the result of a compromise

between the effects of potential distribution in the double layer and slower electron transfer rates as the separation between the electrode and the reaction site increases; a high value of γ would force most of the electron transfers to take place very close to the electrode where ϕ_r is more negative, also leading to low rate constants.

Rate constants for the reduction of TCNE$^-$ in the presence of LiClO$_4$ and NaClO$_4$ were faster than those in the presence of TBAF or TEAP. Presumably this means that the OHP is very close to the electrode in the alkali perchlorate electrolytes, as one would expect from the small crystal radii of the cations, and this must outweigh the decrease in electron transfer rate usually observed when strong ion pairing with cations takes place [10,19,26].

Effect of Electrode Material

The rate constants for TCNE$^-$ reduction are higher at carbon than at platinum (Table 3). This is unlikely to be due simply to less negative values of ϕ_2 at the carbon electrode since those at platinum are already very small. The cause is probably different solvent adsorption on the two materials. Electron transfers in acetonitrile have been found to be faster at mercury than at platinum, and blockage of the platinum surface by adsorbed acetonitrile was suggested as one possibility [24]. There is strong evidence, both from capacitance measurements [35] and from in-situ infrared spectra [48], that a platinum surface in acetonitrile is covered with a layer of chemisorbed acetonitrile molecules, while this does not appear to be the case for mercury electrodes [49,50]. If acetonitrile is not strongly adsorbed

on carbon, as seems likely, the same argument might apply here. It is probable, however, that the OHP at carbon is closer to the electrode surface than is the OHP at platinum, because the electrolyte ions are prevented from reaching the platinum surface by the chemisorbed layer. Then any of the above arguments for slower electron transfer with increasing electrode-OHP distance would apply here also.

CONCLUSIONS

(1) $TCNE^{2-}$ and $TCNQ^{2-}$ form strongly bound contact ion pairs with alkali metal cations in acetonitrile, while $TCNE^{\bar{}}$ and $TCNQ^{\bar{}}$ do not. Ion pairing is stonger for Li^+ than for Na^+ and stronger for $TCNE^{2-}$ than for $TCNQ^{2-}$.

(2)   The standard heterogeneous rate constant for reduction of $TCNE^{\bar{}}$ decreases as the size of the electrolyte cation increases, and is larger at carbon than at platinum.   Both of these effects are probably due to a dependence of electron transfer rate on the metal-OHP separation, which may be at least partly the result of nonadiabatic electron transfer.   The reductions of TCNQ, $TCNQ^{\bar{}}$, and TCNE are reversible up to 500 mV s^{-1}, which argues for a high inner reorganization energy in the reduction of $TCNE^{\bar{}}$.   These conclusions are rather tentative in view of the relative lack of information about the double layer at these electrodes in acetonitrile.   More information will be obtained by measurement of all the rate constants for these systems.

Acknowledgement

References

1. M.R. Suchanski and R.P. Van Duyne J. Am. Chem. Soc. 98 (1976) 250.

2. M.E. Peover Trans. Faraday Soc. 60 (1964) 417.

3. M.E. Peover Trans. Faraday Soc. 58 (1962) 2370.

4. M. Sharp Electrochim. Acta 21 (1976) 973.

5. M. Sharp J. Electroanal. Chem. 88 (1978) 193.

6. D.L. Jeanmaire, M.R. Suchanski and R.P. Van Duyne
   J. Am. Chem. Soc. 97 (1975) 1699.

7. D.L. Jeanmaire and R.P. Van Duyne J. Am. Chem. Soc. 98 (1976)
   4029.

8. S. Pons, S.B. Khoo, J. Janata, S.W. Feldberg, J.K. Foley and
   A.S. Hinman Electrochim. Acta 30 (1985) 569.

9. S.B. Khoo, S. Pons, J. Janata, S.W. Feldberg, J.K. Foley and
   A.S. Hinman Electrochim. Acta 30 (1985) 575.

10. C. Russel and W. Jaenicke J. Electroanal. Chem. 199 (1986) 139.

11. T. Nagaoka, S. Okazaki and T. Fujinaga J. Electroanal. Chem. 133
    (1982) 89.

12. M.E. Peover and J.D. Davies J. Electroanal. Chem. 6 (1963) 46.

13. J.S. Jaworski and M.K. Kalinowski J. Electroanal. Chem. 76 (1977)
    301.

14. A. Lasia and M.K. Kalinowski J. Electroanal. Chem. 36 (1972) 511.

15. T. Nagaoka and S. Okazaki J. Electroanal. Chem. 158 (1983) 139.

16. S. Pons, S.B. Khoo, A. Bewick, M. Datta, J.J. Smith, A.S. Hinman
    and G. Zachmann J. Phys. Chem. 88 (1984) 3575.

17. J.E. Mulvaney, R.J. Cramer and H.K. Hall, Jr. J. Polymer Sci. 21
    (1983) 209.

18. C. Russel and W. Jaenicke Z. Phys. Chem., NF, 139 (1984) 97.

19. C. Russel and W. Jaenicke J. Electroanal. Chem. 180 (1984) 205.

20. B.S. Jensen, A. Ronlan and V.D. Parker Acta Chem. Scand. B 29
    (1975) 394.

21. A.J. Fry, C.S. Hutchins and L.L. Chung J. Am. Chem. Soc. 97 (1975) 591.

22. B.S. Jensen and V.D. Parker J. Am. Chem. Soc. 97 (1975) 5211

23. A. Baranski and W.R. Fawcett J. Electroanal. Chem. 100 (1979) 185.

24. D.A. Corrigan and D.H. Evans J. Electroanal. Chem. 106 (1980) 287.

25. W.R. Fawcett and A. Lasia J. Phys. Chem. 89 (1985) 5695.

26. W.R. Fawcett and A. Lasia J. Phys. Chem. 82 (1978) 1114.

27. A.J. Fry, Synthetic Organic Electrochemistry, Harper and Row, New York, 1972, p. 72.

28. H. Lund and P. Iverson in Organic Electrochemistry, M. Baizer, Ed., Marcel Dekker, New York, 1969, p.57.

29. A.R. Siedle, G.A. Candela and J.F. Finnegan Inorg. Chim. Acta 35 (1979) 125.

30. J. Jacq Electrochim. Acta. 12 (1967) 311.

31. I. Ruzic and D.E. Smith J. Electroanal. Chem. 58 (1975) 145.

32. R.S. Nicholson Anal. Chem. 37 (1965) 1351.

33. Equation (21) was obtained by combining equations (6.3.10) and (6.3.11) in A.J. Bard and L.R. Faulkner "Electrochemical Methods", Wiley, New York, 1980.

34. A.J. Bard and L.R. Faulkner "Electrochemical Methods", Wiley, New York, 1980, Chapter 12.

35. O.A. Petrii and I.G. Khomchenko J. Electroanal. Chem. 106 (1980) 277.

36. L.R. Melby, R.T. Hardner, W.R. Hertler, W. Mahler, R.E. Benson and W.E. Mochel J. Am. Chem. Soc. 84 (1962) 3374.

37. R.H. Wopshall and I. Shain Anal. Chem. 39 (1967) 1514.

38. J.M. Hale in "Reactions of Molecules at Electrodes", (Ed) N.S. Hush, p.229, Wiley, Interscience, 1971.

39. N.S. Hush Electrochim. Acta 13 (1968) 1005.

40. M.E. Peover, reference 46, p.259.

41. H. Kojima and A.J. Bard J. Am. Chem. Soc 97 (1975) 6317.

42. N. Sutin and B.S. Brunschwig ACS Symp. Ser. 198 (1982) 105.

43. M.D. Newton ACS Symp. Ser. 198 (1982) 255.

44. M.D. Newton and N. Sutin Ann. Rev. Phys. Chem. 35 (1984) 437.

45. J.T. Hupp and M.J. Weaver J. Electroanal. Chem. 152 (1983) 1.

46. J.T. Hupp, H.Y. Liu, J.K. Farmer, T. Gennet and M.J. Weaver
     J. Electroanal. Chem. 168 (1984) 313.

47. J.T. Hupp and M.J. Weaver J. Phys. Chem. 88 (1984) 1463.

48. T. Davidson, S. Pons, A. Bewick and P.P. Schmidt J. Electroanal.
     Chem. (1981) 237.

49. R.Gambert and H. Baumgartel J. Electroanal. Chem. 183 (1985) 315.

50. W.R. Fawcett and R.O. Loufty Can. J. Chem. 51 (1972) 230.

Figure Legends

Figure 1. Cyclic voltammograms for reduction of TCNQ (1.00 mM in
acetonitrile, 0.1 M supporting electrolyte) at glassy
carbon with different supporting electrolytes.
Sweep rate 100 mV s^{-1}.

Figure 2. Cyclic voltammograms for reduction of TCNE (1.00 mM in
acetonitrile, 0.1 M supporting electrolyte) at glassy carbon
with different supporting electrolytes.
Sweep rate 100 mV s^{-1}.

Figure 3. Cyclic voltammograms for reduction of TCNE (1.00 mM in
acetonitrile) with mixtures of supporting electrolytes.
 (i) Pt electrode, 0.095 M TBAF + 0.005 M LiClO$_4$
 (ii) Pt electrode, 0.05 M TEAP + 0.05 M LiClO$_4$
 (iii) C electrode, 0.05 M TBAF + 0.05 M LiClO$_4$
All at 100 mV s^{-1}.

Table 1: Peak potentials and peak separations for the first and second reduction waves of TCNQ (1.00 mM) at 100 mV s^{-1}.

Electrode	Electrolyte	First Wave			Second Wave		
		$-E_{pc}$ (V)	$-E_{pa}$ (V)	ΔE_p (mV)	$-E_{pc}$ (V)	$-E_{pa}$ (V)	ΔE_p (mV)
Carbon	TBAF	0.140	0.072	68	0.691	0.627	64
	NaClO$_4$	0.146	0.080	66	0.659	0.597	62
	LiClO$_4$	0.146	0.082	64	0.551	0.490	61
Platinum	TBAF	0.140	0.077	63	0.695	0.628	70
	TEAP	0.144	0.079	65	0.695	0.629	66
	NaClO$_4$	0.145	0.072	67	0.660	0.592	68
	LiClO$_4$	0.140	0.078	68	0.558	0.498	60

Table 2: Peak potentials and peak separations for the first and second reduction waves of TCNE (1.00 mM) at 100 mV s^{-1}.
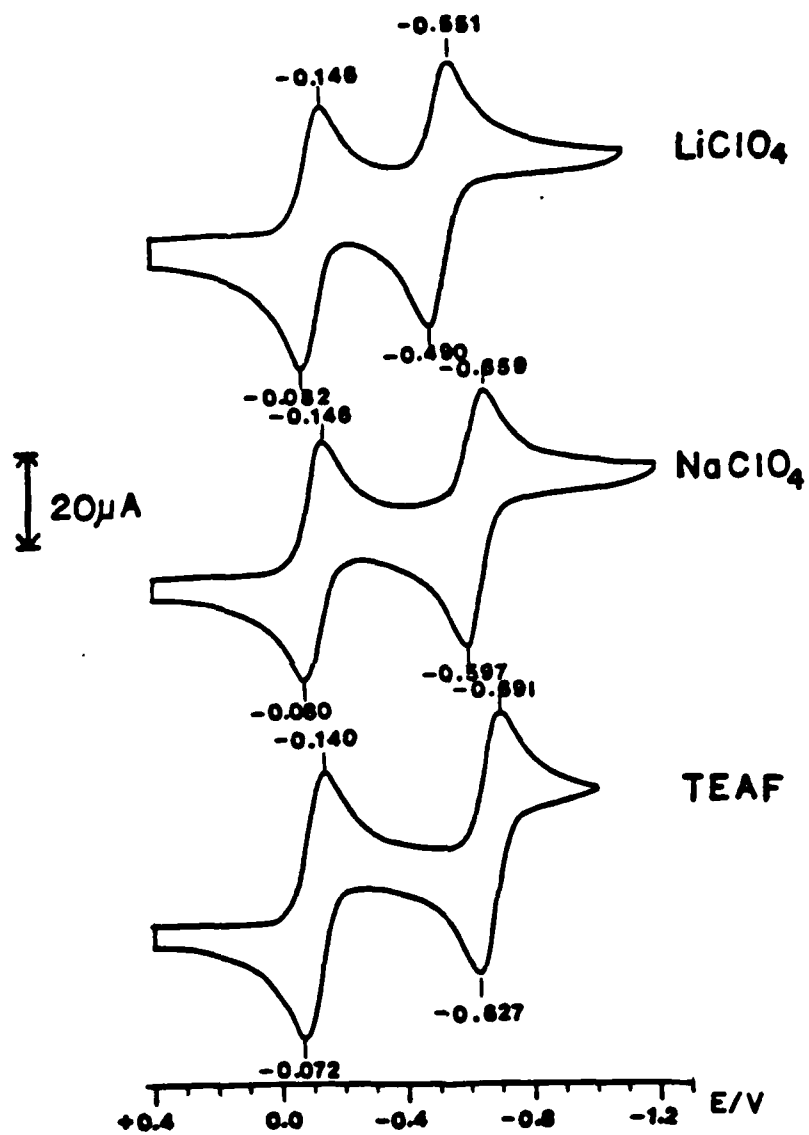
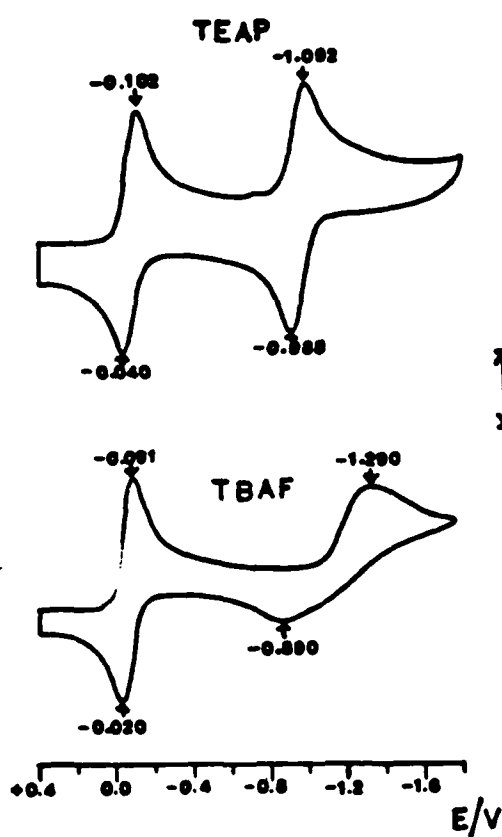| Electrode	Electrolyte	First Wave			Second Wave		
		$-E_{pc}$ (V)	$-E_{pa}$ (V)	ΔE_p (mV)	$-E_{pc}$ (V)	$-E_{pa}$ (V)	ΔE_p (mV)
Carbon	TBAF	0.091	0.020	71	1.290	0.890	400
	TEAP	0.102	0.040	59	1.092	0.988	94
	NaClO$_4$	0.102	0.041	61	0.981	0.909	72
	LiClO$_4$	0.114	0.052	62	0.840	0.753	87
Platinum	TBAF	0.110	0.038	72	1.625	1.100	525
	TEAP	0.105	0.042	63	1.264	0.967	297
	NaClO$_4$	0.110	0.042	68	0.980	0.907	73
	LiClO$_4$	0.108	0.045	63	0.833	0.756	77

Table 3: Thermodynamic and kinetic data for reduction of TCNQ and TCNE: half-wave potentials for first reduction waves and second reduction waves, and standard heterogeneous rate constants for second reduction wave at carbon (k_S^C), platinum (k_S^{Pt}), and platinum after correction for double layer effects ($k_{S,cor}^{Pt}$).

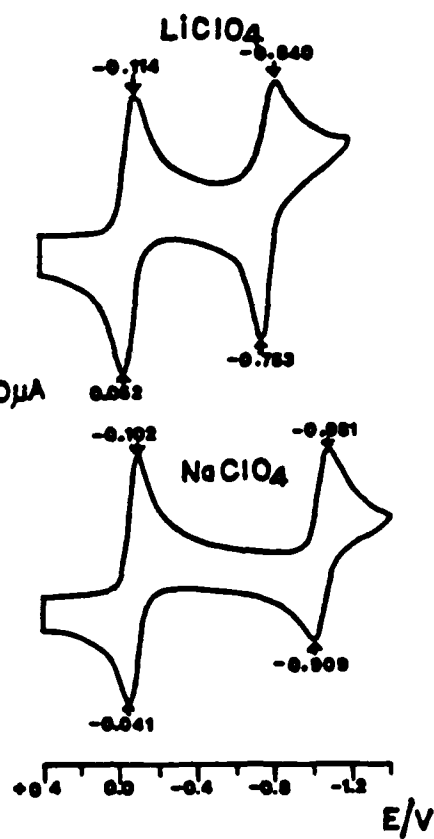| Substrate	Cation	$-E_{\frac{1}{2}}^{(1)}$ (V)	$-E_{\frac{1}{2}}^{(2)}$ (V)	k_S^C (cm s^{-1})	k_S^{Pt} (cm s^{-1})	$k_{S,cor}^{Pt}$ (cm s^{-1})
TCNQ	TBA$^+$	-0.11	-0.66	reversible[a]	reversible	>0.08
	TEA$^+$	-0.11	-0.66	reversible	reversible	>0.08
	Na$^+$	-0.11	-0.63	reversible	reversible	>0.06
	Li$^+$	-0.11	-0.52	reversible	reversible	>0.05
TCNE	TBA$^+$	-0.07	-1.05[b]	1.1×10^{-3}	0.7×10^{-5}	6×10^{-5}
	TEA$^+$	-0.07	-1.05	1.0×10^{-2}	1.5×10^{-3}	0.01
	Na$^+$	-0.07	-0.94	reversible	reversible	>0.18
	Li$^+$	-0.07	-0.79	reversible	reversible	>0.10

a. $k_S > 3 \times 10^{-2}$ cm s^{-1} for reversible systems
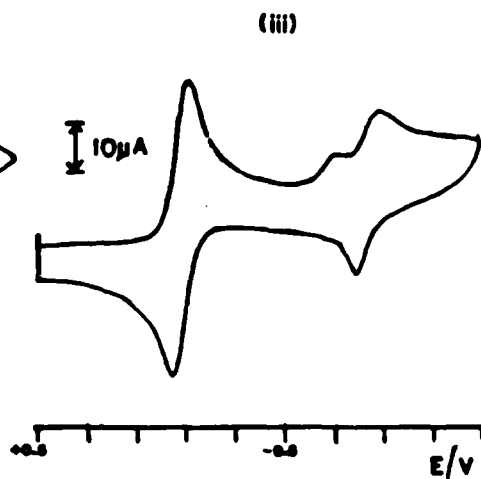b. assumed equal to $E_{1/2}$ for TCNE/TEAP system

LiClO₄

NaClO₄

20μA

TEAF

E/V

TEAP

−0.162 −1.052

−0.040 −0.586

LiClO₄

−0.714 −0.649

0.052 −0.753

TBAF

−0.061 −1.290

−0.020 −0.890

NaClO₄

−0.162 −0.661

−0.041 −0.609

20μA

+0.4   0.0   −0.4   −0.8   −1.2   −1.6   E/V

+0.4   0.0   −0.4   −0.8   −1.2   E/V

⑤

(i)   (ii)   (iii)
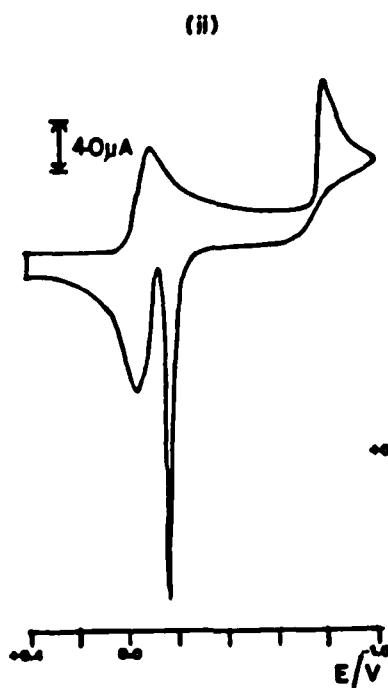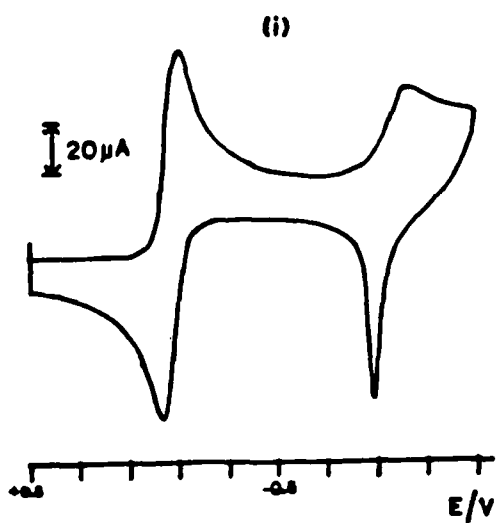
TECHNICAL REPORT DISTRIBUTION LIST, GEN

	No. Copies		No. Copies
Office of Naval Research Attn: Code 413 800 N. Quincy Street Arlington, Virginia 22217	2	Dr. David Young Code 334 NORDA NSTL, Mississippi 39529	1
Dr. Bernard Douda Naval Weapons Support Center Code 5042 Crane, Indiana 47522	1	Naval Weapons Center Attn: Dr. Ron Atkins Chemistry Division China Lake, California 93555	1
Commander, Naval Air Systems Command Attn: Code 310C (H. Rosenwasser) Washington, D.C. 20360	1	Scientific Advisor Commandant of the Marine Corps Code RD-1 Washington, D.C. 20380	1
Naval Civil Engineering Laboratory Attn: Dr. R. W. Drisko Port Hueneme, California 93401	1	U.S. Army Research Office Attn: CRD-AA-IP P.O. Box 12211 Research Triangle Park, NC 27709	1
Defense Technical Information Center Building 5, Cameron Station Alexandria, Virginia 22314	12	Mr. John Boyle Materials Branch Naval Ship Engineering Center Philadelphia, Pennsylvania 19112	1
DTNSRDC Attn: Dr. G. Bosmajian Applied Chemistry Division Annapolis, Maryland 21401	1	Naval Ocean Systems Center Attn: Dr. S. Yamamoto Marine Sciences Division San Diego, California 91232	1
Dr. William Tolles Superintendent Chemistry Division, Code 6100 Naval Research Laboratory Washington, D.C. 20375	1		

ABSTRACTS DISTRIBUTION LIST, 359/627

Dr. Paul Delahay
Department of Chemistry
New York University
New York, New York 10003

Dr. E. Yeager
Department of Chemistry
Case Western Reserve University
Cleveland, Ohio 44106

Dr. P. J. Hendra
Department of Chemistry
University of Southampton
Southampton SO9 5NH
United Kingdom

Dr. C. E. Mueller
The Electrochemistry Branch
Naval Surface Weapons Center
White Oak Laboratory
Silver Spring, Maryland 20910

Dr. J. Driscoll
Lockheed Palo Alto Research
  Laboratory
3251 Hanover Street
Palo Alto, California 94304

Dr. Sam Perone
Chemistry & Materials
  Science Department
Lawrence Livermore National Laboratory
Livermore, California 94550

Dr. D. N. Bennion
Department of Chemical Engineering
Brigham Young University
Provo, Utah 84602

Dr. Royce W. Murray
Department of Chemistry
University of North Carolina
Chapel Hill, North Carolina 27514

Dr. R. A. Marcus
Department of Chemistry
California Institute of Technology
Pasadena, California 91125

Dr. B. Brummer
EIC Incorporated
111 Downey Street
Norwood, Massachusetts 02062

Dr. J. J. Auborn
Bell Laboratories
Murray Hill, New Jersey 07974

Dr. Adam Heller
Bell Laboratories
Murray Hill, New Jersey 07974

Dr. Joseph Singer, Code 302-1
NASA-Lewis
21000 Brookpark Road
Cleveland, Ohio 44135

Dr. A. B. Ellis
Chemistry Department
University of Wisconsin
Madison, Wisconsin 53706

Dr. P. P. Schmidt
Department of Chemistry
Oakland University
Rochester, Michigan 48063

Library
Duracell, Inc.
Burlington, Massachusetts 01803

Dr. Manfred Breiter
Institut fur Technische Elektrochemie
Technischen Universitat Wien
9 Getreidemarkt, 1160 Wien
AUSTRIA

Electrochimica Corporation
20 Kelly Court
Menlo Park, California 94025-1418

ABSTRACTS DISTRIBUTION LIST, 359/627

Dr. M. Wrighton
Chemistry Department
Massachusetts Institute
  of Technology
Cambridge, Massachusetts 02139

Dr. B. Stanley Pons
Department of Chemistry
University of Utah
Salt Lake City, Utah 84112

Donald E. Mains
Naval Weapons Support Center
Electrochemical Power Sources Division
Crane, Indiana 47522

S. Ruby
DOE (STOR)
Room 5E036 Forrestal Bldg., CE-14
Washington, D.C. 20595

Dr. A. J. Bard
Department of Chemistry
University of Texas
Austin, Texas 78712

Dr. Janet Osteryoung
Department of Chemistry
State University of New York
Buffalo, New York 14214

Dr. Donald W. Ernst
Naval Surface Weapons Center
Code R-33
White Oak Laboratory
Silver Spring, Maryland 20910

Mr. James R. Moden
Naval Underwater Systems Center
Code 3632
Newport, Rhode Island 02840

Dr. Bernard Spielvogel
U.S. Army Research Office
P.O. Box 12211
Research Triangle Park, NC 27709

Dr. Aaron Fletcher
Naval Weapons Center
Code 3852
China Lake, California 93555

Dr. M. M. Nicholson
Electronics Research Center
Rockwell International
3370 Miraloma Avenue
Anaheim, California

Dr. Michael J. Weaver
Department of Chemistry
Purdue University
West Lafayette, Indiana 47907

Dr. R. David Rauh
EIC Laboratories, Inc.
111 Downey Street
Norwood, Massachusetts 02062

Dr. Aaron Wold
Department of Chemistry
Brown University
Providence, Rhode Island 02192

Dr. Martin Fleischmann
Department of Chemistry
University of Southampton
Southampton SO9 5NH ENGLAND

Dr. R. A. Osteryoung
Department of Chemistry
State University of New York
Buffalo, New York 14214

Dr. John Wilkes
Air Force Office of Scientific
  Research
Bolling AFB
Washington, D.C. 20332

Dr. R. Nowak
Naval Research Laboratory
Code 6171
Washington, D.C. 20375

Dr. D. F. Shriver
Department of Chemistry
Northwestern University
Evanston, Illinois 60201

ABSTRACTS DISTRIBUTION LIST, 359/627

Dr. Hector D. Abruna
Department of Chemistry
Cornell University
Ithaca, New York 14853

Dr. A. B. P. Lever
Chemistry Department
York University
Downsview, Ontario M3J1P3

Dr. Stanislaw Szpak
Naval Ocean Systems Center
Code 633, Bayside
San Diego, California 95152

Dr. Gregory Farrington
Department of Materials Science
 and Engineering
University of Pennsylvania
Philadelphia, Pennsylvania 19104

M. L. Robertson
Manager, Electrochemical
 and Power Sources Division
Naval Weapons Support Center
Crane, Indiana 47522

Dr. T. Marks
Department of Chemistry
Northwestern University
Evanston, Illinois 60201

Dr. Micha Tomkiewicz
Department of Physics
Brooklyn College
Brooklyn, New York 11210

Dr. Lesser Blum
Department of Physics
University of Puerto Rico
Rio Piedras, Puerto Rico 00931

Dr. Joseph Gordon, II
IBM Corporation
5600 Cottle Road
San Jose, California 95193

Dr. Nathan Lewis
Department of Chemistry
Stanford University
Stanford, California 94305

Dr. D. H. Whitmore
Department of Materials Science
Northwestern University
Evanston, Illinois 60201

Dr. Alan Bewick
Department of Chemistry
The University of Southampton
Southampton, SO9 5NH ENGLAND

Dr. E. Anderson
NAVSEA-56Z33 NC #4
2541 Jefferson Davis Highway
Arlington, Virginia 20362

Dr. Bruce Dunn
Department of Engineering &
  Applied Science
University of California
Los Angeles, California 90024

Dr. Elton Cairns
Energy & Environment Division
Lawrence Berkeley Laboratory
University of California
Berkeley, California 94720

Dr. Richard Pollard
Department of Chemical Engineering
University of Houston
Houston, Texas 77004

Dr. M. Philpott
IBM Corporation
5600 Cottle Road
San Jose, California 95193

Dr. Donald Sandstrom
Boeing Aerospace Co.
P.O. Box 3999
Seattle, Washington 98124

Dr. Carl Kannewurf
Department of Electrical Engineering
  and Computer Science
Northwestern University
Evanston, Illinois 60201

Dr. Joel Harris
Department of Chemistry
University of Utah
Salt Lake City, Utah 84112

ABSTRACTS DISTRIBUTION LIST, 359/627

Dr. Robert Somoano
Jet Propulsion Laboratory
California Institute of Technology
Pasadena, California 91103

Dr. Edward Fletcher
Department of Mechanical Engineering
University of Minnesota
Minneapolis, Minnesota 55455

Dr. Johann A. Joebstl
USA Mobility Equipment R&D Command
DRDME-EC
Fort Belvoir, Virginia 22060

Dr. John Fontanella
Department of Physics
U.S. Naval Academy
Annapolis, Maryland 21402

Dr. Judith H. Ambrus
NASA Headquarters
M.S. RTS-6
Washington, D.C. 20546

Dr. Martha Greenblatt
Department of Chemistry
Rutgers University
New Brunswick, New Jersey 08903

Dr. Albert R. Landgrebe
U.S. Department of Energy
M.S. 6B025 Forrestal Building
Washington, D.C. 20595

Dr. John Wasson
Syntheco, Inc.
Rte 6 - Industrial Pike Road
Gastonia, North Carolina 28052

Dr. J. J. Brophy
Department of Physics
University of Utah
Salt Lake City, Utah 84112

Dr. Walter Roth
Department of Physics
State University of New York
Albany, New York 12222

Dr. Charles Martin
Department of Chemistry
Texas A&M University
College Station, Texas 77843

Dr. Anthony Sammells
Eltron Research Inc.
4260 Westbrook Drive, Suite 111
Aurora, Illinois 6C505

Dr. H. Tachikawa
Department of Chemistry
Jackson State University
Jackson, Mississippi 39217

Dr. C. A. Angell
Department of Chemistry
Purdue University
West Lafayette, Indiana 47907

Dr. Theodore Beck
Electrochemical Technology Corp.
3935 Leary Way N.W.
Seattle, Washington 98107

Dr. Thomas Davis
Polymer Science and Standards
  Division
National Bureau of Standards
Washington, D.C. 20234

Dr. Farrell Lytle
Boeing Engineering and
  Construction Engineers
P.O. Box 3707
Seattle, Washington 98124

Ms. Wendy Parkhurst
Naval Surface Weapons Center R-33
R-33
Silver Spring, Maryland 20910

Dr. Robert Gotscholl
U.S. Department of Energy
MS G-226
Washington, D.C. 20545

OL/413/83/01
359/413-2

ABSTRACTS DISTRIBUTION LIST, 359/627

Dr. John Owen
Department of Chemistry and
   Applied Chemistry
University of Salford
Salford M5 4WT ENGLAND

Dr. Boone Owens
Department of Chemical Engineering
   and Materials Science
University of Minnesota
Minneapolis, Minnesota 55455

Dr. J. O. Thomas
University of Uppsala
Institute of Chemistry
Box 531
S-751 21 Uppsala, Sweden

Dr. O. Stafsudd
Department of Electrical Engineering
University of California
Los Angeles, California 90024

Dr. S. G. Greenbaum
Department of Physics
Hunter College of CUNY
New York, New York 10021

Dr. Menahem Anderman
W.R. Grace & Co.
Columbia, Maryland 20144

END

DATE
FILMED
7-88
DTIC